Journal of Anatomy

J. Anat. (2011) **218**, pp163–172 doi: 10.1111/j.1469-7580.2010.01313.x

Peripheral nerve regeneration in the MRL/MpJ ear wound model

Gemma Buckley,[1] Anthony D. Metcalfe[1,2] and Mark W. J. Ferguson[1,2]

[1]*Faculty of Life Sciences, UK Centre for Tissue Engineering, University of Manchester, Manchester, UK*
[2]*Renovo Group plc, Manchester, UK*

Abstract

The MRL/MpJ mouse displays an accelerated ability to heal ear punch wounds without scar formation (whereas wounds on the dorsal surface of the trunk heal with scar formation), offering a rare opportunity for studying tissue regeneration in adult mammals. A blastema-like structure develops and subsequently the structure of the wounded ear is restored, including cartilage, skin, hair follicles and adipose tissue. We sought to assess if the MRL/MpJ strain also possessed an enhanced capacity for peripheral nerve regeneration. Female MRL/MpJ and C57BL/6 mice were wounded with a 2-mm excisional biopsy punch to the centre of each ear and two 4-mm excisional biopsy punches to the dorsal skin. Immunohistochemical dual staining of pan-neurofilament and CD31 markers was used to investigate reinnervation and vascularisation of both the dorsal surface of the trunk and ear wounds. The MRL/MpJ mouse ear exhibited a significantly ($P > 0.01$) higher density of regenerated nerves than C57BL/6 between 10 and 21 days post-wounding when the blastema-like structure was forming. Unlike dorsal skin wounds, nerve regeneration in the ear wound preceded vascularisation, recapitulating early mammalian development. Immunohistochemical data suggest that factors within the blastemal mesenchyme, such as aggrecan, may direct nerve regrowth in the regenerating ear tissue.

Key words ear; nerve; regeneration; skin.

Introduction

The MRL/MpJ mouse, originally developed as a model for lupus erythromatosis, displays a rare ability amongst mammals in that it has the capacity to heal injured ear tissue without scar formation. A biopsy punch wound to the centre of the mouse ear appears to heal by a process of regeneration rather than normal adult wound repair and bears several histological similarities to amphibian limb regeneration and late embryogenesis (Clark et al. 1998; Rajnoch et al. 2003; Colwell et al. 2006; Echeverri & Tanaka, 2003; for review see Stocum, 2004). Histological analysis of the MRL/MpJ ear wound has revealed the formation of a blastema-like structure at 14 days post-wounding, from which hair follicles, sebaceous glands, cartilage, blood vessels and skin have the capacity to fully regenerate (Rajnoch et al. 2003; Metcalfe & Ferguson, 2005, 2007; Metcalfe et al. 2006). In amphibian regeneration studies, a blastema is defined by the presence of a proliferative mass of mesenchymal progenitor cells, which accumulate at the injury site and subsequently redifferentiate to give rise to new structures, for example, the replacement of a severed limb (Tanaka, 2003; Stocum, 2004). Mammalian regeneration research remains under-investigation, partly due to the fact that exemplar model systems are rare but such models are increasingly being championed to play a major role in the future of tissue engineering.

Many animal models have been utilised to describe the reinnervation of skin post-wounding (Hsieh et al. 1996; Stankovic et al. 1996). Peripheral nerves possess a very limited regenerative ability, particularly following a nerve section rather than nerve crush injuries where reinnervation is more successful (Navarro et al. 1997). Reinnervation of the correct targets is rarely achieved, often resulting in abnormal sensation (Niessen et al. 1999). From a skin tissue engineering perspective, one of the main goals is to encourage reinnervation of both artificial and autologous skin grafts from the surrounding uninjured host tissue to provide the graft with normal sensation. The enhanced healing capacity of the MRL/MpJ mouse ear, where the original architecture of the injured tissue is completely restored, has been well documented. However, no reports have investigated the capacity of peripheral nerve regeneration within this mammalian model, or if in fact the peripheral nerve

Correspondence
Professor Mark W. J. Ferguson, Renovo, Core Technology Facility, 48 Grafton Street, Manchester M13 9XX, UK. T: +44 (0)161 276 7121; F: +44 (0)161 276 7240; E: mark.ferguson@renovo.com

Accepted for publication *24 September 2010*
Article published online *18 October 2010*

network in the regenerated tissue resembles that of unwounded tissue.

As an initial investigation, we aimed to map the nerve regeneration process during formation of the blastema-like structure and subsequent regeneration of the MRL/MpJ ear. This initial study compares peripheral nerve regeneration in the MRL/MpJ with the C57BL/6 strain, which has previously exhibited a reduced tissue regenerative capacity in the ear wound and has been termed a 'poor healer' (Clark et al. 1998). Rajnoch et al. (2003) were the first to report variation within the MRL/MpJ regenerating model, showing that the outcome of regeneration was partially governed by the degree of trauma imposed. They went on to show that, when a sharp clinical biopsy punch is used instead of a crude punch as used in the study of Clark et al. (1998), the C57BL/6 strain does possess a limited regenerative capacity, displaying some of the histological features observed in the MRL/MpJ ear wound (Rajnoch et al. 2003). These include; re-epithelialisation, dermal extension, angiogenesis, chondrogenesis, folliculogenesis, and myogenesis. Importantly, however, they note that these features were far more pronounced and accelerated in the MRL/MpJ strain, which unlike the C57BL/6 strain went on to fully close the ear punch hole (Rajnoch et al. 2003).

We also mapped the immunolocalisation of various factors, e.g. the neural inhibitory extra cellular matrix molecule aggrecan, which may play a role in guiding the direction of nerve growth through the regenerating tissue with the temporal appearance of the regenerating nerve network. Beare et al. (2006) and Colwell et al. (2006) reported that, in both strains of mice, an excisional wound to the dorsal surface of the trunk heals by repair and undergoes scar formation with no evidence of a blastema-like structure. This allowed us to investigate the pattern of reinnervation and revascularisation of the dorsal trunk wound tissue and compare it with that of the ear.

Materials and methods

Wounding procedure

All procedures involving animals were carried out in accordance with Home Office regulations of the UK 1986 Animals in Scientific Procedures Act, under appropriate project and personal license authority. Female MRL/MpJ and C57BL/6 mice aged between 7 and 12 weeks were used throughout the study. Buprenorphrine (Vetergesic) was administered (100 μL) subcutaneously at 40 min prior to wounding, at a concentration of 3 μg mL^{-1} (Rhodia Organique Fine Ltd, Bristol, UK). Anaesthesia was maintained using a Bain anaesthetic circuit, 2.5% isoflurane in oxygen and nitrous oxide at a flow rate of 2.5 L min^{-1}. Mice were wounded with a 2-mm full-thickness hole punched through the centre of each ear using a sterile clinical biopsy punch (Stiefel Laboratories, Woodburn Green, UK). Following wounding to the ears, two full-thickness 4-mm punch biopsy excisional wounds were made to the dorsum. The wounds were not sutured, but left to heal by primary intention.

Tissue processing

Mice were killed using CO_2 followed by cervical dislocation at days 7, 10, 14, 21, 35, 84 and 200 post-wounding (n = 6 per time-point for each strain). Skin and ear wounds were excised, bisected, cryo-preserved in optimum cutting temperature embedding matrix (Cell Path, Powys, Wales, UK) and cryo-sectioned (7 μm). Samples of sections from each wound were stained with Masson's trichrome.

Dual-labelling immunohistochemistry

In order to visualise both peripheral nerves and blood vessels on the same tissue section, we executed a dual-labelling protocol. Cryo-sections were rehydrated in 0.1% polyoxyethylenesorbitan monoalurate (Tween-20®) in phosphate-buffered saline (PBST) for 10 min. Sections were placed in a light-excluding humidified chamber and incubated in goat serum block (10% serum, 5% bovine serum albumin in phosphate-buffered saline) for 1 h at room temperature (RT). The serum block was tapped off the slide and the sections were incubated overnight at 4 °C with a rabbit polyclonal cocktail to neurofilaments (NA1297; Biomol) diluted 1 : 500 in serum block. Following incubation, the slides were washed in three changes of PBST for 15 min, and biotinylated anti-rabbit (BA1001, Vector) secondary antibody diluted in serum block (2.5 μg mL^{-1}) was applied to the sections (200 μL per slide) and incubated for 1 h at RT. Sections were washed in three changes of PBST for 15 min and incubated in the dark for 40 min at RT in streptavidin-conjugated fluorescein label (Chemicon, CA, USA) applied at a concentration of 2.5 μg mL^{-1}. The slides were again rinsed in three changes of PBST for 15 min excluding light. The rat monoclonal antibody to CD31 (553370, BD Biosciences) was then applied to the sections (2 μg mL^{-1}) for 1 h at RT in a humidified chamber, followed by rinsing the slides in three changes of PBST for 15 min excluding light. A secondary tetramethyl rhodamine isothiocyanate-conjugated donkey anti-rat antibody (712 025 153, Jackson Immuno Research Labs) was applied to the sections (1.5 μg mL^{-1}), incubated for a further 1 h at RT in a humidified chamber, and again rinsed in three changes of PBST for 15 min excluding light. Finally, sections were mounted in Gelvatol before visualisation.

For dual labelling with a rabbit polyclonal cocktail to neurofilaments (NA1297, Biomol) and a rabbit polyclonal to aggrecan (AB1030, Chemicon), rhodamine red-X-conjugated goat anti-rabbit IgG fab fragments (J111-297-003, Jackson Immuno Research Labs) were used to mask the identity of the anti-aggrecan antibody. As above, rehydrated sections were placed in a light-excluding humidified chamber and incubated in the goat serum block (10% serum, 5% bovine serum albumin in phosphate-buffered saline) for 1 h at RT. The serum block was tapped off the slide and the sections were incubated overnight at 4 °C with the anti-aggrecan antibody diluted in serum block (2.5 μg mL^{-1}). Following incubation, the slides were washed in three changes of PBST for 15 min and the sections were incubated in an excess of fab fragments for 1 h at RT. Following a further three washes in three changes of PBST for 15 min, sections were incubated in anti-pan-neurofilament antibody as described above.

Masson's trichrome histology

Rehydrated sections were immersed in filtered Harris's haematoxylin for 4 min, and rinsed in running tap water for 5 min until the sections appeared blue in colour. The sections were placed in 1% (v/v) picric acid solution for 30 s and rinsed in water. Slides were transferred to 0.1% (w/v) Biebrich scarlet for 1 min, dipped in water and immersed in 50% phosphomolybdic acid/50% phosphotungstic acid for 10 min. Finally, slides were placed in 2.5% (w/v) fast green for 6 min. Following rinsing in water, sections were rapidly dehydrated in graded alcohols (50–100%) and then in two changes of xylene for 10 min each, before being mounted in Pertex™ (CellPath, Newton, Powys, UK).

Quantification of nerve regeneration in the ear wound

Images were captured and processed with a Spot RT Slider Digital camera with a 1 × magnification lens and Spot RT-v.3.5 software running on a silicon graphics Pentium III 230 MHz PC (Diagnostic Instruments Inc., MI, USA). Images were subsequently transferred into Adobe Photoshop version 7.0 as JPEG files, where they were later analysed, montaged or quantified depending on the type of staining. The extent of nerve regeneration into the ear wound blastema-like structure was quantified using the image-analysis software package Image ProPlus (version 4.1.0.0; Media Cybernetics) measured as the percentage of positive staining within a defined area of the blastema. The final measurement was taken from an average of six different mice for each time-point for each of the individual strains. For each mouse an average of three samples taken 150 μm apart through the centre of the ear wound was calculated. All quantified data were tested for significance with non-parametric one-way ANOVAS using Prism software (Version 3.02; GraphPad Software Inc.).

Results

Histological analysis of the MRL/MpJ ear wound

Dual-staining immunohistochemistry for pan-neurofilament and CD31 revealed that the ear was highly innervated and well vascularised. The intricate nature of the axonal network and innervation of target structures such as hair follicles is revealed in Fig. 1. There was no noticeable difference in innervation between the MRL/MpJ and C57BL/6 strains. The staining technique was validated by the incorporation of negative controls during the dual-staining procedure. Figure 2A,B demonstrates the histological orientation of the proximal and distal ear wound margins sampled for this study. The architecture of the proximal and distal wound margins is shown in the Masson's trichrome-stained histological section in Fig. 2C. A blastema-like structure was apparent in the proximal MRL/MpJ wound at 14 days post-wounding, evident by the presence of a bulbous mass of proliferating cells, surrounded by a thickened epithelium. Large epidermal downgrowths protruding into the mesenchyme, often in direct alignment with the cut cartilage stump, were visible.

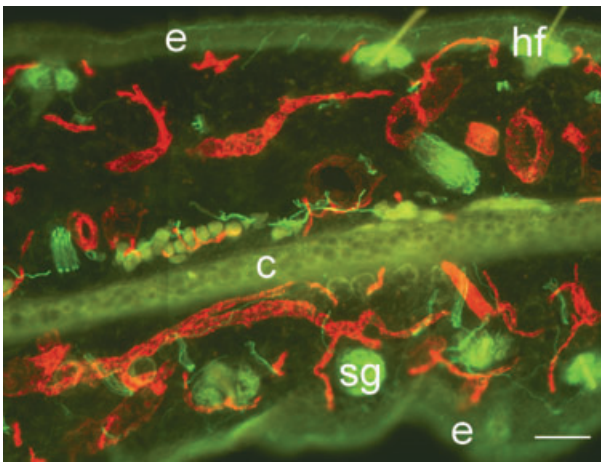

Fig. 1 Innervation and vascularisation of the murine ear. Dual immunohistochemical staining for pan-neurofilament (fluorescein isothiocyanate) and CD31 (tetramethyl rhodamine isothiocyanate) shows extensive innervation and vascularisation in unwounded ear skin (30-μm section) of the MRL/MpJ mouse. Autofluorescence shows structures such as epidermis (e), hair follicles (hf), cartilage layer (c) and sebaceous glands (sg). Scale bar = 100 μm.

The distal wound margin tended to heal at a slower rate than the proximal wound margin. We also confirmed the findings of other studies (Clark et al. 1998; Heber-Katz, 1999; Rajnoch et al. 2003) indicating that, although C57BL/6 ear wounds displayed some regenerative features of a blastema-like structure including epithelial downgrowths, myogenesis and chondrogenesis, such features were far less prominent and the wounds failed to fully regenerate and close.

Peripheral nerve regeneration in the MRL/MpJ blastema-like structure

In order to determine if the MRL/MpJ strain displayed a significantly greater capacity than the C57BL/6 strain for peripheral nerve regeneration in the wounded ear, the density of neurofilament-positive nerves within the blastema-like structure was quantified at various times during the healing process. Figure 3 represents the percentage area of positive staining in a defined area of the blastema-like structure. Analysis of unwounded ear skin revealed no significant difference in the extent of innervation between the two strains. Following wounding, nerve regeneration initiated at 7 days post-wounding and nerve density in the regenerating tissue gradually increased. As reported in previous studies (Clark et al. 1998; Rajnoch et al. 2003), between days 14 and 21 post-wounding the MRL/MpJ proximal blastema-like structure underwent extensive proliferation with a progressively larger annular swelling healing at a faster rate than the C57BL/6 strain. The MRL/MpJ strain exhibited a higher proximal wound nerve density compared with C57BL/6 throughout the whole time-course,

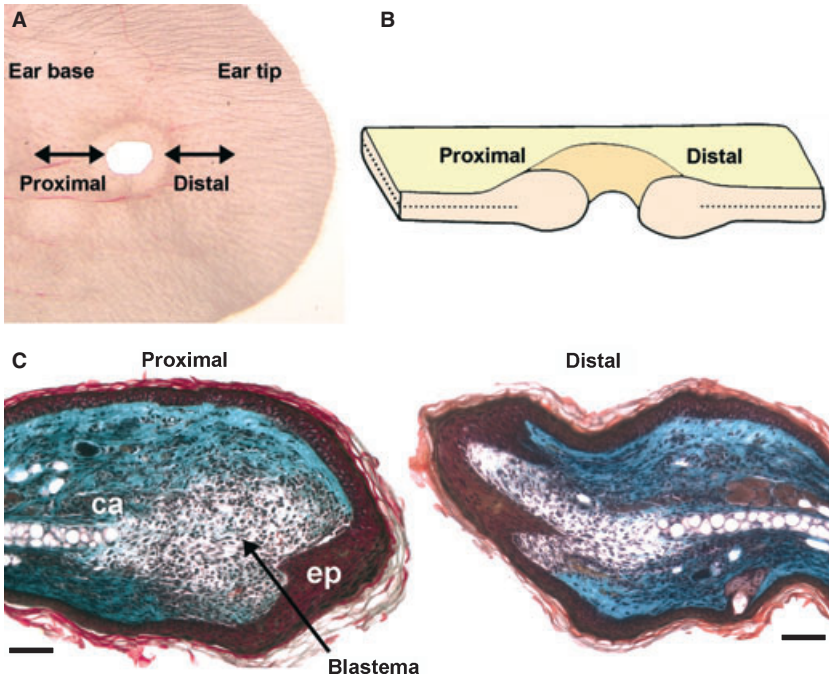

Fig. 2 Orientation of the proximal and distal wound margins of the ear punch hole. Ear wounds were harvested at regular time-points up to 200 days post-wounding. Ear tissue was sectioned laterally (A,B) to orientate both proximal and distal wound margins on the same slide as demonstrated by the section through the centre of the ear wound at 14 days post-wounding stained with Masson's trichrome (C) showing the cartilage layer (ca) and epithelial downgrowth (ep). Nuclei stained purple/black, muscle, red blood cells, fibrin and cytoplasmic granules stained orange/red, and collagen stained light green. Scale bars = 100 μm.

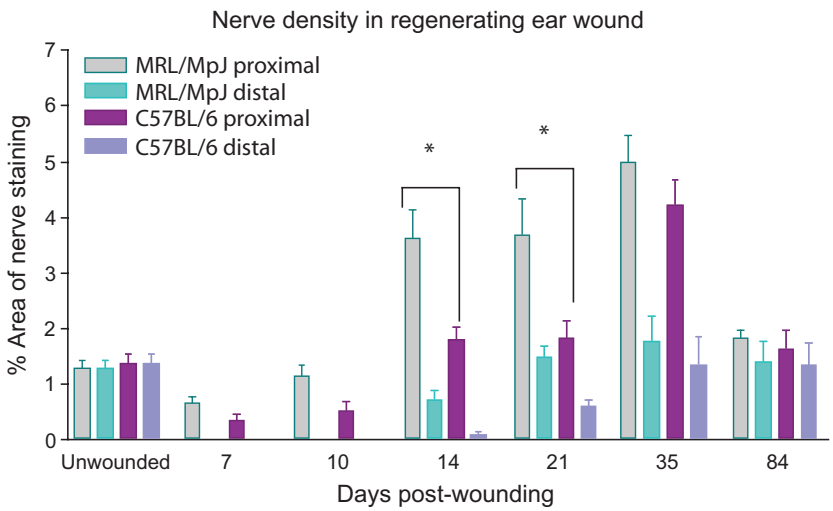

Fig. 3 Comparison of nerve regenerative capacity in both MRL/MpJ and C57BL/6 ear wounds. Mouse ears were wounded with a 2-mm biopsy punch and harvested at days 7, 10, 14, 21, 35 and 84 post-wounding. Immunohistochemistry was used to detect expression of pan-neurofilament within the regenerating blastema-like structure. The density of regenerating nerves within the blastema-like structure of both proximal and distal wound margins was quantified using image-analysis software and expressed as the percentage of the area positively stained. Data shown represent means + SEM, $n = 6$ for each time-point and strain. There was a significantly higher density of regenerated nerves in the proximal blastema than the distal blastema across the whole experimental time-course in both strains ($P < 0.01$). The MRL/MpJ strain exhibited a period of hyperinnervation in the proximal blastema with a significantly higher nerve density ($P < 0.05$*) at days 14 and 21 compared with C57BL/6, indicating that the MRL/MpJ has an accelerated nerve regenerative capacity in the ear. Nerve density peaks in both the proximal and distal blastema at 35 days post-wounding with both strains showing a similar density. By day 84 nerve density reduced in both strains returning to levels observed in unwounded skin. *Statistically significant.

demonstrating a significant difference at days 14 and 21 ($n = 6$, $P < 0.05$) (Fig. 3). There was no noticeable difference in revascularisation of the healing ear wound between the two strains.

At day 14 post-wounding, multiple nerve fibre growth infiltrated the developing proximal blastema-like structure followed by new blood vessels in both strains (Fig. 4). Furthermore, regenerating nerves were observed to migrate towards the downgrowth of the thickened epithelial tip ahead of the onset of vascularisation of the regenerating structure. The area immediately adjacent to the cut cartilage was devoid of nerve ingrowth. These features were

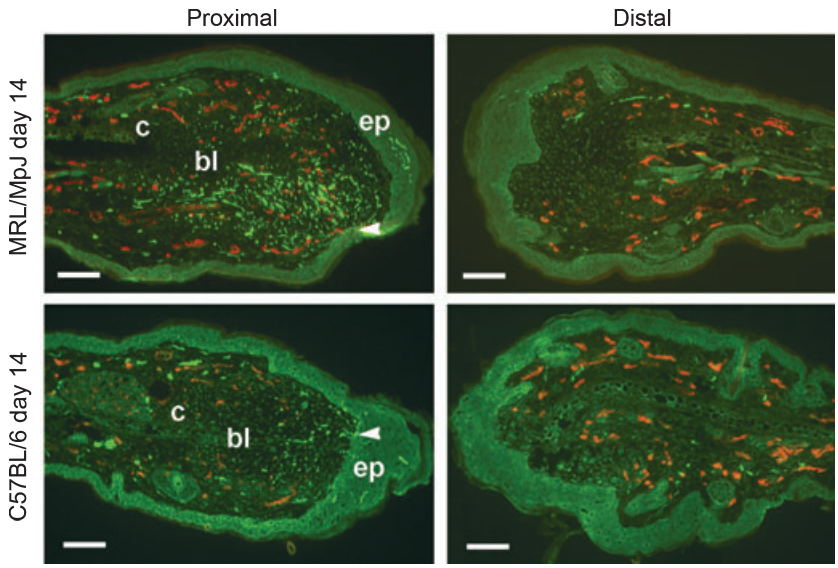

Fig. 4 Reinnervation and vascularisation of healing ear wounds at 14 days post-wounding. Mice were wounded with a 2-mm biopsy punch and harvested at 14 days post-wounding. Dual immunohistochemical staining for pan-neurofilament (fluorescein isothiocyanate, green) and CD31 (tetramethyl rhodamine isothiocyanate, red) was used to detect nerve and blood vessel regeneration in both proximal and distal wound margins. Hyperinnervation was observed in proximal MRL/MpJ blastema with greater nerve density compared with the C57BL/6 strain. In both strains, nerve regeneration precedes vascularisation and regenerating nerve fibres grow towards epithelial downgrowths (ep, arrowheads) but avoid growing immediately in line with the cut edge of the cartilage (c) at the centre of the blastema-like structure (bl). Distal wound margins display lower numbers of nerves. Scale bars = 100 μm.

also observed in the C57BL/6 proximal wound margin, but the extent of innervation was reduced (Fig. 4). In both strains the distal wound margin was less developed than the proximal wound margin, and this was reflected by reduced nerve and blood vessel regeneration observed in the distal margin of both strains (Figs 3 and 4). The difference in nerve density between proximal and distal wounds was found to be significantly different ($n = 6$, $P < 0.01$) in both strains up to day 84 post-wounding (Fig. 4).

Following a period of hyperinnervation peaking at day 35, nerve density in both strains returned to a level similar to that of normal/unwounded ear skin by day 84 post-wounding. It is important to note, however, that, although there was no significant difference in nerve density between the strains at day 84 post-wounding, the outcome of healing was very different. By this time the opposing blastema edges in the MRL/MpJ had fused to form a continuous layer of regenerated skin and regenerating cartilage. The C57BL/6 ear wound, however, remained open and appeared to have ceased regenerating by day 84 post-wounding. The cartilage layer remained capped with a bulbous aggregate of cartilage in the C57BL/6 animals. Fusion of opposing margins also failed to occur and levels of neurofilament-positive nerves in both proximal and distal wound margins reduced dramatically to resemble that of unwounded ear skin (Fig. 3).

A major morphological distinction between the two strains was the fusion of opposing epithelial margins in the MRL/MpJ as the ear wound closed at around 84 days post-wounding (Fig. 5). Figure 5 represents a series of tissue sections at the point of MRL/MpJ ear wound closure and demonstrates a pattern of continued nerve regeneration as the epithelial margins fused to form a continuous layer. Following fusion and breakdown of the partitioning margins, pioneering nerve fibres from the proximal margin protrude through into the distal blastema area (Fig. 5A). Tissue sections sampled from deeper within the regenerating tissue extending towards the wound edge showed what appeared to be a mixing of the opposing axon clusters (Fig. 5B). At a distance from the centre of the hole where regeneration was nearly complete, there was evidence of cartilage islands fusing to form a continuous layer, as well as the emergence of hair follicles (Fig. 5C). In this region, the level of innervation had decreased and shared a similar appearance with unwounded skin.

These results confirm that nerve regeneration does occur within the blastema-like structure of the MRL/MpJ regenerating ear, and at an accelerated rate compared with C57BL/6. However, it cannot be concluded that the regenerated nerve network was fully functional. Analysis of fully regenerated MRL/MpJ ear wounds harvested at 84 days post-wounding showed the emergence of a *de-novo* cartilage layer, hair follicles, sebaceous glands and a significant pruning of the regenerated nerve network (Fig. 5C). Detailed examination of hair follicles sampled from the centre of this regenerated tissue revealed that they were intricately innervated and vascularised (Fig. 6), suggesting that the regenerated nerve fibres had reached their target organs.

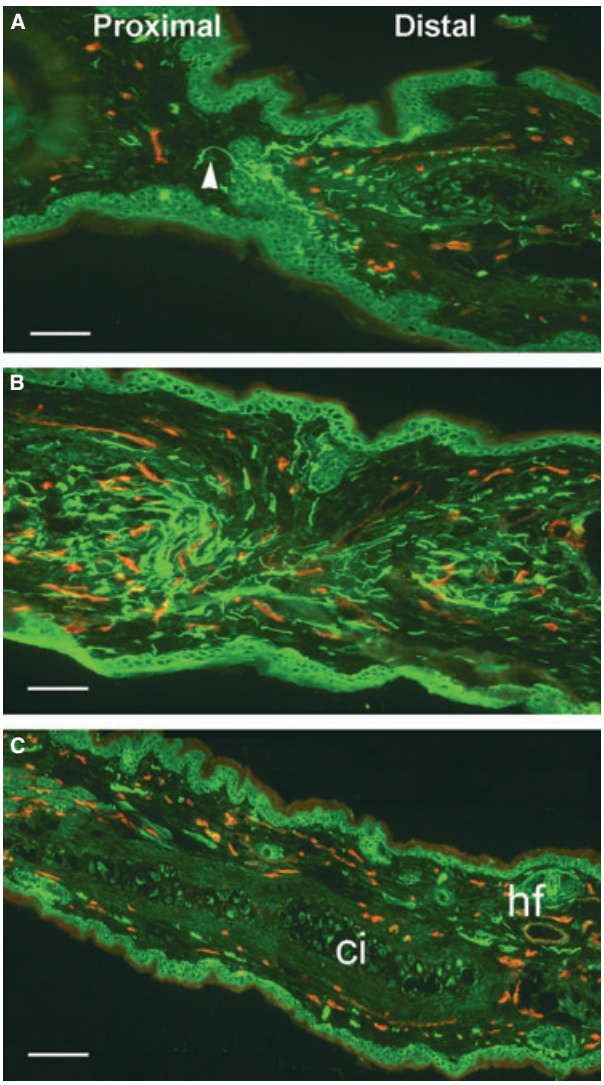

Fig. 5 Reinnervation and vascularisation of MRL/MpJ ear at 84 days post-wounding. Sequential sections through the centre of an ear wound (A) show fusion of opposing epithelial margins and penetration of pioneer regenerating nerve fibres (arrowhead) from the proximal into distal blastema. (B) Disintegration of dividing epithelium and further infiltration of regenerating nerves from the proximal wound margin accompanied by new blood vessels. Away from the centre of the wound where tissue regeneration was nearly complete (C) evident from fusion of cartilage islands (ci) and emergence of hair follicles (hf), nerve and blood vessel density notably decreased, resembling that of an unwounded mouse ear. Scale bars = 100 μm.

Inhibition of nerve infiltration in the MRL/MpJ blastema-like structure

Dual staining for both pan-neurofilament and aggrecan revealed strong aggrecan deposition localised around the cut cartilage (data not shown). As the MRL/MpJ blastema-like structure elongated into a cone shape at around day 35 post-wounding, aggrecan deposition became confined to a thin strip progressing from the cut cartilage out towards

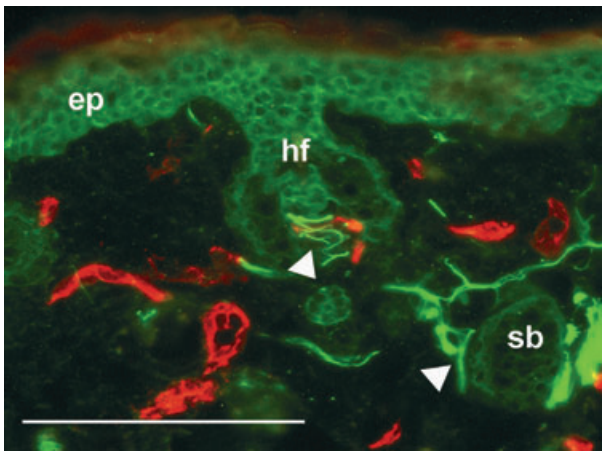

Fig. 6 Innervation of hair follicles in newly regenerated MRL/MpJ ear tissue. Dual immunohistochemical staining for pan-neurofilament (fluorescein isothiocyanate, green) and CD31 (tetramethyl rhodamine isothiocyanate, red) of the MRL/MpJ mouse ear at 84 days post-wounding. Autofluorescence shows structures such as epidermis (ep), hair follicles (hf) and sebaceous glands (sb). Arrowheads show innervation of target structures within the newly regenerated tissue of the MRL/MpJ ear wound. Scale bar = 100 μm.

the wound epithelium (Fig. 7). Histological analysis of blastema sections from day 35 post-wounding onwards showed evidence of cartilage regeneration within this area, with the emergence of cellular condensations similar to those described by Fell (1925) in chick limb buds.

Figure 7 illustrates the emergence of cartilage islands forming within the strip of aggrecan deposition between the original cartilage edges. Once the cartilage islands had formed it was noted that they themselves then became a source of intense aggrecan deposition, stretching even further out into the regenerating ear tissue. A magnified view of the cartilage island (Fig. 7) (also highlighted with haematoxylin and eosin staining) showed that axons continued to avoid this area and appeared to track along the periphery of aggrecan deposition avoiding the path of cartilage island extension.

Capacity and nature of peripheral nerve regeneration in the dorsal skin wound

As also reported in previous publications (Metcalfe & Ferguson, 2005; Beare et al. 2006; Colwell et al. 2006), an excisional cutaneous wound to the skin of the dorsal trunk of the MRL/MpJ mouse results in fibrosis and scar formation, whereas an ear wound is capable of tissue regeneration. Figure 8A shows a Masson's trichrome-stained MRL/MpJ dorsal wound section at 7 days post-wounding undergoing the normal mammalian wound repair process. Immunohistochemical analysis of pan-neurofilament and CD31 within the wound revealed that the area had already become hypervascularised by as early as day 7 post-wounding.

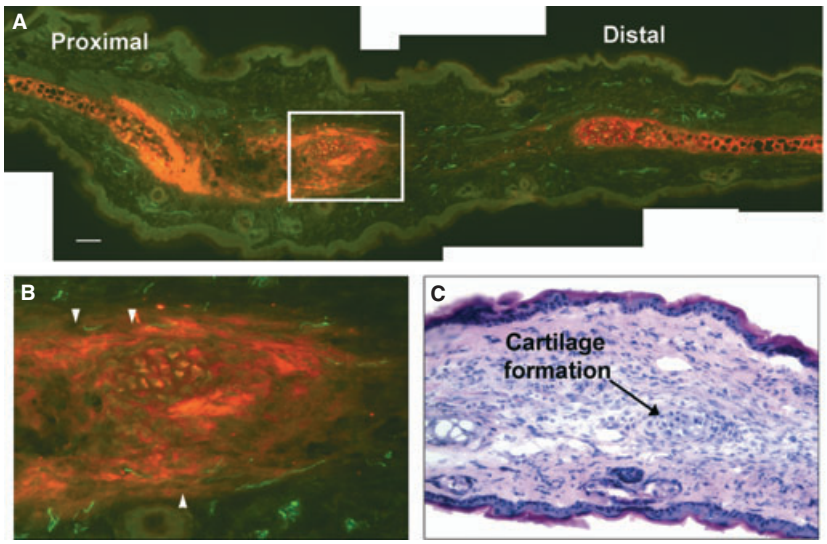

Fig. 7 Aggrecan expression in the regenerating MRL/MpJ ear at 84 days post-wounding when the opposing wound margins had fused. Aggrecan localisation was found at both wound margins but was particularly strong at the cartilage edge of the proximal margin (A). Expression was also concentrated around a developing cartilage island (highlighted by white box). (B) Magnification of the cartilage island reveals nerves regenerating along the border of the dense aggrecan localisation around the growing cartilage island (arrowheads). Haematoxylin and eosin staining reveals the pre-cartilage condensation at the centre of the aggrecan expression, indicating cartilage island formation (C). Scale bar = 100 μm.

However, peripheral nerve regeneration was only found in the outer regions of the wound where nerve fibres had begun to sprout into the wound area from surrounding healthy tissue (Fig. 8B).

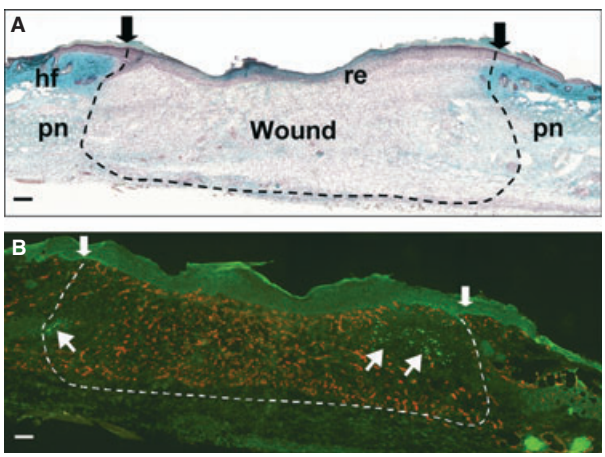

Fig. 8 Innervation and vascularisation of MRL/MpJ dorsal skin excisional wounds. Masson's trichrome-stained section of a day 7 full-thickness dorsal skin wound (A) depicts wound area (arrows and dotted line), re-epithelialisation of wound (re), excised panniculus (pn) and surrounding hair follicles (hf). Immunohistochemical dual staining for pan-neurofilament (fluorescein isothiocyanate, green) and CD31 (tetramethyl rhodamine isothiocyanate, red) was used to detect regeneration of nerves and blood vessels into the wound. At 7 days post-wounding (B), blood vessels were the first to form in the wound area followed by only a few nerve fibres from the periphery (arrows). Scale bars = 100 μm.

Discussion

Regeneration of peripheral nerves following a cut injury is known to occur with limited success during adult mammalian wound repair, leading to a considerable loss of functional recovery. The MRL/MpJ model offers an opportunity to elucidate the subtle mechanisms governing peripheral nerve regeneration in both an environment that leads to scar formation, such as cutaneous wounds to the dorsal surface of the trunk, and an environment in which new fully innervated tissue is regenerated via a blastema-like structure. This study provides the first histological account of peripheral nerve regeneration within the MRL/MpJ ear wound.

At 14 days post-wounding when the characteristic blastema-like structure became apparent, the proximal wound margin of the MRL/MpJ began to show a significantly accelerated peripheral nerve regeneration capacity compared with the C57BL/6 strain. It is not known why the MRL/MpJ mouse should possess an increased ability to regenerate nerves in the ear, or whether this phenomenon is linked to the different healing capacities observed in the two strains studied. It has been well documented that, with one biopsy punch wound made to the centre of the ear, the MRL/MpJ strain demonstrates an accelerated capacity for tissue regeneration and ear hole closure compared with the C57BL/6 strain. Importantly, unlike the MRL/MpJ wounds, none of the C57BL/6 ear wounds closed.

Nerve and blood supply is more abundant near the base of the ear (i.e. near the proximal wound margin), with large axon bundles and vessels becoming more finely branched

towards the ear tip. In order to innervate the distal wound margin, regenerating nerves at the base of the ear have to track around the large hole created by the biopsy punch. This may account for why the rate of innervation of the distal wound margin appeared slower than in the proximal wound in both strains.

Peripheral nerves are known to be vital for limb regeneration in Urodele amphibians (Singer, 1952). Furthermore, this regeneration can be stimulated by either motor or sensory fibres, providing that there is a high enough density of nerves present at the initiation of blastema formation (Singer, 1952). The mitogenic factor of epimorphic regeneration is thought to be released by the regenerating nerves but as yet remains unidentified, although fibroblast growth factor (Gospodarowicz & Mescher, 1980), transferrin (Munaim & Mescher, 1986), substance P (Smith et al. 1995) and, more recently, the newt anterior gradient protein family member newt anterior gradient (Kumar et al. 2007; Yin & Poss, 2008) have all been proposed as potential candidates. It is therefore feasible that the greater abundance of regenerating nerves present at the MRL/MpJ ear wound compared with the C57BL/6 mice promotes enhanced tissue regeneration by releasing a higher concentration of the mitogenic factor(s).

It is not thought that the MRL/MpJ mouse possesses an intrinsically enhanced capacity for peripheral nerve regeneration as preliminary studies indicate that no apparent difference was observed in the rate of innervation of dorsal wounds between the two strains. It seems that the enhanced nerve regeneration capacity may be localised to the ear wound. It is also possible that factors generated within the MRL/MpJ blastema-like structure itself may have a greater ability to attract regenerating nerves into the wound site. Tonge & Leclere (2000) demonstrated that a diffusible factor(s) released from the regenerating limb blastema of an axolotl was capable of stimulating the growth of primary sensory axons *in vitro.*

In light of the current data presented here it is possible that the thickened epithelial layer observed in the MRL/MpJ, and to a lesser extent in C57BL/6, secretes neurotrophic factors that stimulate nerve regeneration into the blastema. In all MRL/MpJ mice sampled, the regenerating nerves infiltrated the growing blastema-like structure avoiding the centre of the mesenchymal ear structure before streaming towards the thickest part of the wound epithelium, particularly at either side of the epithelial downgrowths. In some cases, the nerves grew directly into this thickened epithelium. This suggests that the nerves may be attracted into the blastema and towards the wound epidermis by an as yet unidentified neurotrophic factor(s). Further investigations will be required to establish if neurotrophic factors are present at the interface between wound epidermis and mesenchyme and also to ascertain if expression levels of these factors vary between MRL/MpJ and C57BL/6 strains.

In the MRL/MpJ excisional dorsal trunk skin wounds, the formation of scar tissue resulted in a healed wound devoid of both hair follicles and sebaceous glands with patches of unorganised regenerated nerves remaining throughout the underlying granulation tissue. The outcome of healing in the regenerated MRL/MpJ ear wound, however, was very different. Following a period of hyperinnervation, hair follicles and sebaceous glands within the regenerated ear tissue subsequently showed vascularisation and intricate patterns of innervation, similar to unwounded skin. Although it cannot be concluded that the regenerated nerve network had regained functionality, this frequent observation strongly suggests that, within the ear wound environment, nerves are able to undergo appropriate path-finding and innervate their new target appendages.

This study revealed an interesting difference in the pattern of nerve regeneration between ear and dorsal skin wounds. In the ear wounds of both strains, regenerating axons infiltrated the blastema structure before angiogenesis occurred. This observation recapitulates the process of early fetal development where nerves precede blood vessel growth and are thought to play a role in arterial patterning of the developing vascular network (Mukouyama et al. 2002). It is not apparent from the published literature if this is also the case for regenerating amphibian limb blastemas. Using *ErbB3*$^{+/+}$ mice that lack Schwann cells associated with peripheral nerves, Mukouyama et al. (2002) revealed that, in the absence of Schwann cells, the pattern of axon growth was highly disorganised, but also that the association and alignment of blood vessels with these nerves were greatly reduced. Therefore, in skin it appears that the branching pattern of peripheral nerves provides a template that directs the branching of an emerging arterial network. In direct contrast, blood vessel infiltration precedes reinnervation in the dorsal skin wounds. Consistent with this observation, numerous reinnervation studies including skin flaps (Manek et al. 1993), keratodermal autografts (Gu et al. 1994, 1995) and excisional dorsal wounds in CD1 mice (Henderson et al. 2006) report that peripheral nerves normally regenerate into the healing tissue only after it has been re-epithelialised and revascularised, and that sensory fibres appear first (Manek et al. 1993; Terenghi, 1995).

The distinct difference in nerve and blood vessel infiltration between ear and dorsal wounds revealed in this study may be linked to the difference in their modes of healing. This study supports the current thinking that the MRL/MpJ blastema-like structure in the ear is more embryonic in its mechanism of healing, whereas the dorsal wound follows the classic mode of adult repair (Metcalfe & Ferguson, 2007). Unlike wounds in loose dorsal skin, the ear skin is double sided and connected to the cartilage via tightly adhering tissue. There is no wound bed in the ear and therefore, unlike repair, skin contracture cannot occur as the hole is devoid of a fibrin clot, provisional matrix or granulation tissue. Neither can epithelial migration of

opposing wound margins occur. The mouse ear is effectively a layer of cartilaginous tissue covered on both sides, e.g. a thin dermis and epithelium; this thin structure may enable the establishment of diffusion gradients similar to a developing embryonic limb.

The path of nerve infiltration appeared to be spatially organised in relation to other structures within the ear tissue. A very similar pattern of innervation was demonstrated in amputated *Xenopus* limb blastemas by Suzuki et al. (2005) where multiple regenerating axons grew around the outer edges of the blastema avoiding the centre before converging beneath the wound epidermis. In both the MRL/MpJ and C57BL/6, an elliptical-shaped area of the mesenchyme directly in line with the cut edge of the cartilage remained devoid of both nerves and blood vessels. Further investigation using dual-antigen immunohistochemistry for aggrecan and pan-neurofilament revealed a concentrated area of aggrecan deposition in this region, which remained avascular and devoid of nerves.

Expression of aggrecan indicates the presence of cartilage cell precursors (chondroblasts). This was visible in the MRL/MpJ ear wound as pre-cartilage cellular aggregates emerged within the band of aggrecan deposition at day 84 post-wounding. Johnson et al. (2002, 2005) demonstrated that human intervertebral disc aggrecan inhibits both endothelial cell adhesion and neurite extension, and repels sensory neurite growth cones. This may account for why regenerating axons were found at the outer edge of the MRL/MpJ blastema where aggrecan staining appeared more diffuse. However, it is important to note that such assumptions are purely speculative and based on correlations and comparisons with other experimental models. Further investigation is required to establish the expression pattern of aggrecan in other mouse models, and determine if aggrecan isolated from the MRL/MpJ blastema-like structure is also capable of inhibiting vascular and neuronal cell growth *in vitro*.

Summary

Following an ear punch wound, MRL/MpJ mice display an enhanced peripheral nerve regeneration capacity compared with the poorer healing strain C57BL/6. The pattern of reinnervation and vascularisation of the ear wound is more reminiscent of fetal development in that nerves infiltrate the blastema ahead of regenerating blood vessels. MRL/MpJ mouse ear regeneration parallels histological and immunocytochemical events identified in amphibian limb regeneration and mammalian fetal development. The MRL/MpJ mouse model of regeneration offers an opportunity to investigate the molecular and cellular basis of adult mammalian scar-free skin regeneration. A greater understanding of the mechanisms of peripheral nerve regeneration within the MRL/MpJ mouse ear and the importance of these nerves in the regeneration process is warranted.

References

Beare AH, Metcalfe AD, Ferguson MWJ (2006) Location of injury influences the mechanisms of both regeneration and repair within the MRL/MpJ mouse. *J Anat* **209**, 547–559.

Clark LD, Clark RK, Heber-Katz E (1998) A new murine model for mammalian wound repair and regeneration. *Clin Immunol Immunopathol* **88**, 35–45.

Colwell AS, Krummel TM, Kong W, et al. (2006) Skin wounds in the MRL/MPJ mouse heal with scar. *Wound Repair Regen* **14**, 81–90.

Echeverri K, Tanaka EM (2003) Electroporation as a tool to study *in vivo* spinal cord regeneration. *Dev Dyn* **226**, 418–425.

Fell H (1925) The histogenesis of cartilage and bone in the long bones of embryonic fowl. *J Morphol Physiol* **40**, 417–459.

Gospodarowicz D, Mescher AL (1980) Fibroblast growth factor and the control of vertebrate regeneration and repair. *Ann N Y Acad Sci* **339**, 151–174.

Gu XH, Terenghi G, Purkis PE, et al. (1994) Morphological changes of neural and vascular peptides in human skin suction blister injury. *J Pathol* **172**, 61–72.

Gu XH, Terenghi G, Kangesu T, et al. (1995) Regeneration pattern of blood vessels and nerves in cultured keratinocyte grafts assessed by confocal laser scanning microscopy. *Br J Dermatol* **132**, 376–383.

Heber-Katz E (1999) The regenerating mouse ear. *Semin Cell Dev Biol* **10**, 415–419.

Henderson J, Terenghi G, McGrouther DA, et al. (2006) The reinnervation pattern of wounds and scars may explain their sensory symptoms. *J Plast Reconstr Aesthet Surg* **59**, 942–950.

Hsieh ST, Choi S, Lin WM, et al. (1996) Epidermal denervation and its effects on keratinocytes and Langerhans cells. *J Neurocytol* **25**, 513–524.

Johnson WE, Caterson B, Eisenstein SM, et al. (2002) Human intervertebral disc aggrecan inhibits nerve growth *in vitro*. *Arthritis Rheum* **46**, 2658–2664.

Johnson WE, Caterson B, Eisenstein SM, et al. (2005) Human intervertebral disc aggrecan inhibits endothelial cell adhesion and cell migration *in vitro*. *Spine* **30**, 1139–1147.

Kumar A, Godwin JW, Gates PB, et al. (2007) Molecular basis for the nerve dependence of limb regeneration in an adult vertebrate. *Science* **318**(5851), 772–777.

Manek S, Terenghi G, Shurey C, et al. (1993) Neovascularisation precedes neural changes in the rat groin skin flap following denervation: an immunohistochemical study. *Br J Plast Surg* **46**, 48–55.

Metcalfe AD, Ferguson MWJ (2005) Harnessing wound healing and regeneration for tissue engineering. *Biochem Soc Trans* **33**, 413–417.

Metcalfe AD, Ferguson MWJ (2007) Tissue engineering of replacement skin: the crossroads of biomaterials, wound healing, embryonic development, stem cells and regeneration. *J R Soc Interface* **4**, 413–437.

Metcalfe AD, Willis H, Beare A, et al. (2006) Characterizing regeneration in the vertebrate ear. *J Anat* **209**, 439–446.

Mukouyama YS, Shin D, Britsch S, et al. (2002) Sensory nerves determine the pattern of arterial differentiation and blood vessel branching in the skin. *Cell* **109**, 693–705.

Munaim SI, Mescher AL (1986) Transferrin and the trophic effect of neural tissue on amphibian limb regeneration blastemas. *Dev Biol* **116**, 138–142.

Navarro X, Verdu E, Wendelschafer-Crabb G, et al. (1997) Immunohistochemical study of skin reinnervation by regenerative axons. *J Comp Neurol* **380**, 164–174.

Niessen FB, Spauwen PH, Schalkwijk J, et al. (1999) On the nature of hypertrophic scars and keloids: a review. *Plast Reconstr Surg* **104**, 1435–1458.

Rajnoch C, Ferguson S, Metcalfe AD, et al. (2003) Regeneration of the ear after wounding in different mouse strains is dependent on severity of wound trauma. *Dev Dyn* **226**, 388–397.

Singer M (1952) The influence of the nerve in regeneration of the amphibian extremity. *Q Rev Biol* **27**, 169–200.

Smith MJ, Globus M, Vethamany-Globus S (1995) Nerve extracts and substance P activate the phosphatidylinositol signaling pathway and mitogenesis in newt forelimb regenerates. *Dev Biol* **167**, 239–251.

Stankovic N, Johansson O, Hildebrand C (1996) Regeneration of putative sensory and sympathetic cutaneous nerve endings in the rat foot after sciatic nerve injury. *J Peripher Nerv Syst* **1**, 199–207.

Stocum DL (2004) Amphibian regeneration and stem cells. *Curr Top Microbiol Immunol* **280**, 1–70.

Suzuki M, Satoh A, Ide H, et al. (2005) Nerve-dependent and -independent events in blastema formation during Xenopus froglet limb regeneration. *Dev Biol* **286**, 361–375.

Tanaka EM (2003) Cell differentiation and cell fate during urodele tail and limb regeneration. *Curr Opin Genet Dev* **13**, 497–501.

Terenghi G (1995) Peripheral nerve injury and regeneration. *Histol Histopathol* **10**, 709–718.

Tonge DA, Leclere PG (2000) Directed axonal growth towards axolotl limb blastemas *in vitro*. *Neuroscience* **100**, 201–211.

Yin VP, Poss KD (2008) New regulators of vertebrate appendage regeneration. *Curr Opin Genet Dev* **18**(4), 381–386.